

Adsorption-induced scission of carbon-carbon bonds

Sergei S. Sheiko¹, Frank C. Sun¹, Adrian Randall¹, David Shirvanyants¹, Michael Rubinstein¹, Hyung-il Lee² & Krzysztof Matyjaszewski²

Covalent carbon-carbon bonds are hard to break. Their strength is evident in the hardness of diamonds^{1,2} and tensile strength of polymeric fibres³⁻⁶; on the single-molecule level, it manifests itself in the need for forces of several nanonewtons to extend and mechanically rupture one bond. Such forces have been generated using extensional flow⁷⁻⁹, ultrasonic irradiation¹⁰, receding meniscus¹¹ and by directly stretching a single molecule with nano-probes¹²⁻¹⁶. Here we show that simple adsorption of brush-like macromolecules with long side chains on a substrate can induce not only conformational deformations¹⁷, but also spontaneous rupture of covalent bonds in the macromolecular backbone. We attribute this behaviour to the fact that the attractive interaction between the side chains and the substrate is maximized by the spreading of the side chains, which in turn induces tension along the polymer backbone. Provided the side-chain densities and substrate interaction are sufficiently high, the tension generated will be strong enough to rupture covalent carbon-carbon bonds. We expect similar adsorption-induced backbone scission to occur for all macromolecules with highly branched architectures, such as brushes and dendrimers. This behaviour needs to be considered when designing surface-targeted macromolecules of this type—either to avoid undesired degradation, or to ensure rupture at predetermined macromolecular sites.

A series of brush-like macromolecules with the same number average degree of polymerization of a poly(2-hydroxyethyl methacrylate) backbone, $N_n = 2,150 \pm 100$, and different degrees of polymerization of poly(*n*-butyl acrylate) (pBA) side chains ranging from $n = 12 \pm 1$ to $n = 140 \pm 12$ were synthesized by atom transfer radical polymerization (see 'Polymer Characterization' in the Methods)¹⁸. Owing to the high grafting density, the side chains

repel each other and thereby stretch the backbone into an extended conformation. Placing these macromolecules on a surface enhances the steric repulsion between the side chains, which results in both an extension of the polymer backbone and an increase of the persistence length.

The effect is illustrated in Fig. 1, which shows atomic force microscopy (AFM) micrographs of monolayers of pBA brushes with short (Fig. 1a) and long side chains (Fig. 1b). Measurements on both types of molecules yielded a number average contour length per monomeric unit of the backbone of $l = L_n/N_n = 0.23 \pm 0.02$ nm (see 'Atomic Force Microscopy' in Methods), which is close to $l_0 = 0.25$ nm, the length of the tetrahedral C-C-C section. This means that even for short side chains ($n = 12$), the backbone is already fully extended and adopts an all-*trans* conformation. As the side chains become longer, we observe global straightening of the backbone reflected in the increase of the persistence length (Fig. 1c).

Chain extension requires a substantial amount of force, which we estimate using simple spreading arguments (Fig. 2). Just as in normal liquids, the polymeric side chains spread to cover the higher-energy substrate and thus stretch the macromolecule in all directions. Unlike conventional liquids, however, the spreading of the side chains is constrained by their connection to the backbone. To maximize the number of side chains that adsorb to the substrate, the backbone needs to extend; but even when it is fully elongated, about 50% of the side chains are still not fully in contact with the substrate. In this situation, the attraction of the side chains for the surface causes the polymer backbone to extend beyond its physical limit. Here it is important that the tension imposed by the surface attraction is unevenly distributed over the covalent bonds of the molecular skeleton.

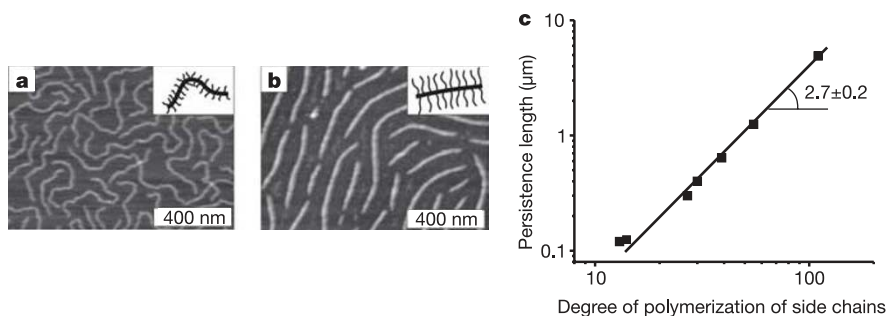


Figure 1 | Conformational response of pBA brush-like macromolecules to adsorption on mica. The conformation of the macromolecules is visualized by AFM, with the light threads in the height images shown in **a** and **b** corresponding to the backbones. The areas between threads are covered by side chains, which cannot be visualized at this scale. With increasing side-

chain length, molecules change from a fairly flexible conformation for $n = 12$ (shown in **a**) to a rod-like conformation for $n = 130$ (shown in **b**). **c**, The persistence length l_p of the adsorbed macromolecules was determined from the statistical analysis of the backbone curvature. It is found to increase with the side chain length as $l_p \propto n^{2.7}$.

¹Department of Chemistry, University of North Carolina at Chapel Hill, Chapel Hill, North Carolina 27599-3290, USA. ²Center for Macromolecular Engineering, Department of Chemistry, Carnegie Mellon University, Pittsburgh, Pennsylvania 15213, USA.

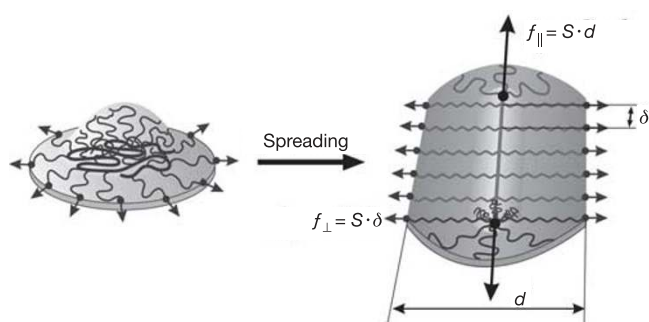


Figure 2 | Schematic of the spreading of a brush-like macromolecule on an attractive substrate. After adsorption, the macromolecule spreads to increase the number of monomeric contacts with the substrate. The brush-like architecture imposes constraints on the spreading process making it anisotropic and leading to extension of the backbone. Along the brush axis, the wetting-induced tensile force $f \approx S \cdot d$ is supported almost entirely by the covalently linked backbone, where S is the spreading coefficient and d is the brush width. In the direction perpendicular to the backbone, the force is evenly distributed over many side chains, each bearing a $f \approx S \cdot \delta$ tensile force, where δ is the distance between the neighbouring side chains.

As shown in Fig. 2, along the brush axis, a major fraction of the wetting-induced tensile force is carried by the backbone; while in the perpendicular direction, the tension is evenly distributed over many side chains. The force at the backbone is estimated as $f \approx S \cdot d$, where S is the spreading coefficient and d is the width of adsorbed brush macromolecules (Fig. 2). Here, we consider only the dominant term in S : that is, the difference between the surface free energies of substrate–gas, liquid–gas, and substrate–liquid–gas interfaces ($S = \gamma_s - \gamma_l - \gamma_{sl}$). Previous measurements for the substrates that were used in this study found $S \approx 20 \text{ mN m}^{-1}$ on graphite¹⁹ and water/alcohol mixtures¹⁷. Therefore, a brush macromolecule with short side chains ($n = 12$) and a width of $d = 11 \text{ nm}$ (ref. 20), is

capable of generating a force of approximately 220 pN on either of these two substrates. This exceeds the typical range of tensile forces of 10–100 pN reported for stretching of individual polymer chains²¹.

According to these arguments, the force value is proportional to the molecule's width and also depends on the surface energy of the substrate. We therefore synthesized pBA brushes with longer side chains ($n = 140$) that would lead to a width of $d = 130 \text{ nm}$ (refs 20, 22); this should result in a tensile force of about 2.6 nN and allow us to challenge the carbon–carbon bonds in the backbone⁹. The molecules were adsorbed on the surface of mica, graphite, silicon wafers and a range of water/propanol mixtures. Whereas molecules on solid substrates could be directly imaged by AFM, the liquid-supported films were first transferred onto a solid substrate using the Langmuir–Blodgett technique and then scanned by AFM (see Methods).

Figure 3a shows a series of AFM images obtained for different incubation times on the water/propanol (99.8/0.2 wt/wt%) substrate, which has a surface energy of $\gamma_s = 69 \pm 1 \text{ mN m}^{-1}$ and a spreading parameter of $S = 21 \pm 2 \text{ mN m}^{-1}$, where the experimental errors are determined by the precision of the Wilhelmy plate method (see 'Langmuir–Blodgett monolayers' in the Methods). As the time spent on the substrate increases, the molecules get progressively shorter while their number density (number of molecules per unit area) correspondingly increases; this suggests scission of the backbone (Fig. 3b). The cumulative length of molecules per unit mass of the material was measured as $\Lambda = \frac{\sum L_i \cdot n_i}{\sigma \times A}$, where n_i is the number of molecules of length L_i within a substrate area A and σ is the Langmuir–Blodgett-controlled mass per unit area of the monolayer. As shown in Fig. 3c, the cumulative length remains approximately constant for different exposure times, supporting the idea that chain scission occurs. Similar observations were made on other substrates (Supplementary Fig. 1). However, we focused on experiments using liquid substrates because they allow gradual variation of the surface energy simply by mixing two different liquids, and because they

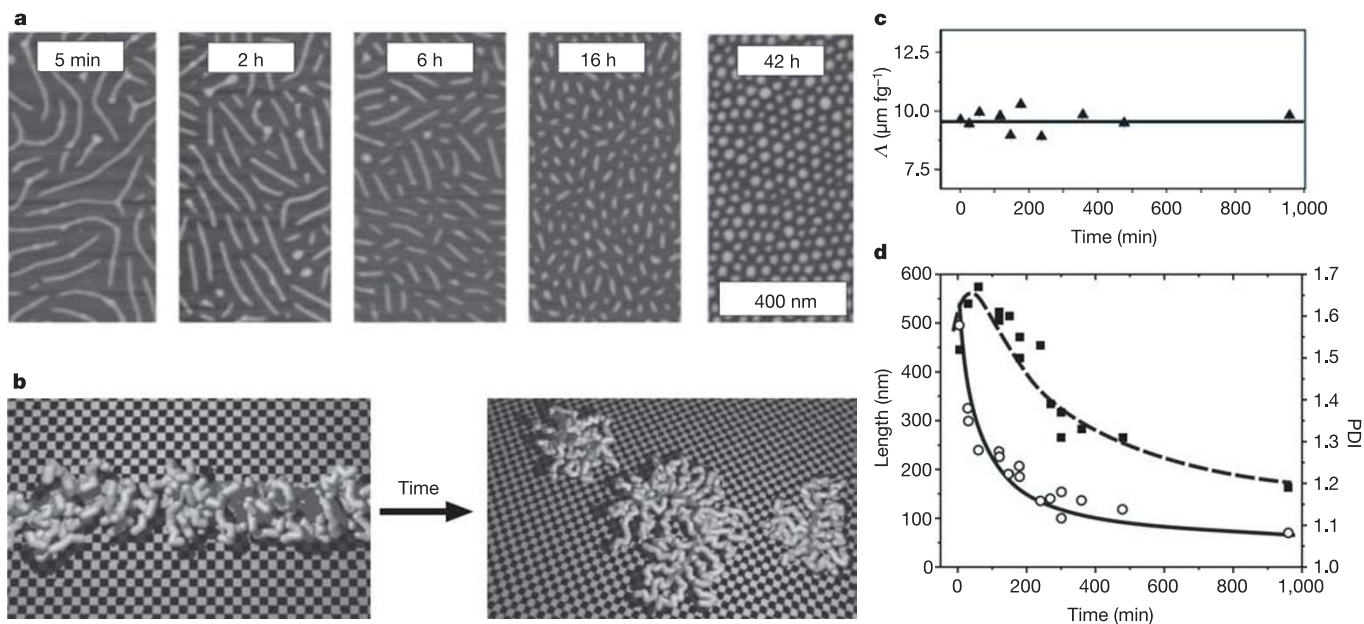


Figure 3 | Adsorption-induced degradation of macromolecules. **a**, The molecular degradation of brush-like macromolecules with long side chains ($n = 140$) on mica was monitored using AFM height imaging after each sample was exposed for different time periods (as indicated in the images) to a water/propanol (99.8/0.2 wt/wt%) substrate. **b**, Schematics of an adsorbed macromolecule (left) which undergoes spontaneous scission of the covalent backbone (right). Side chains are shown in light grey, the backbone in dark grey. **c**, The cumulative length per unit mass, measured within an area of

$A = 25 \mu\text{m}^2$ at a constant mass density of $\sigma = 0.08 \mu\text{g cm}^{-2}$, was found to stay at an approximately constant value of $\Lambda = 9.6 \pm 0.5 \mu\text{m}^2 \text{ fg}^{-1}$ throughout the scission process. **d**, The number average contour lengths measured after different exposure times t (white circles) are fitted according to $\frac{1}{L-L_\infty} = \frac{1}{L-L_0} + \frac{kt}{L_\infty}$, using experimental values for L_0 and L_∞ and a fitted value for k of $2.3 \times 10^{-5} \text{ s}^{-1}$ (solid line). The experimentally determined polydispersity index $\text{PDI} = L_w/L_n$ (black squares) shows good agreement with the computer simulation results of Fig. 4 (dashed line).

facilitate rapid equilibration of the monolayer structure. Both factors ensure reproducibility of the kinetics study discussed below.

Figure 3d shows the characteristic decay of the average molecular length with increasing exposure time of the macromolecules to the water/propanol substrate. To analyse the kinetics of the scission process we assume that the bond scission occurs as a first-order reaction: $B = B_0 e^{-kt}$, where B is the total number of covalent bonds in all backbones within a unit area of the substrate, B_0 is the initial number of bonds at $t = 0$, and k is the rate constant. Because the cumulative length is conserved, we can obtain the number average contour length L from $\frac{1}{L-L_\infty} = \frac{1}{L-L_0} + \frac{kt}{L_\infty}$, where $L_0 = 496 \pm 18$ nm is the initial contour length measured by AFM at $t = 0$ and $L_\infty = 40 \pm 3$ nm is the length of the shortest molecule observed during the scission process (see 'Atomic Force Microscopy' in the Methods). Fitting the experimental data to this equation using k as a fitting parameter yielded $k = 2.3 \times 10^{-5} \text{ s}^{-1}$. That we did not observe molecules shorter than 40 nm even at very long exposure times is because the brush molecules with short backbones adopted star-like morphologies. This ensures that the side chains have more space to spread out and eases tension at the backbone. The reduction of tension prevents further scission, so the above rate equations are applied only at $L \geq L_\infty$.

The scission process seems random, which suggests a uniform distribution of tension along the backbone. We probe this assumption by analysing the length distribution of the system throughout the scission process. As shown in Fig. 3d, the polydispersity index, $\text{PDI} = L_w/L_n$, initially increases and then decays, where L_w and L_n are the weight and number average lengths of adsorbed macromolecules, respectively. This is consistent with random cleavage of backbone C–C bonds, which initially increases the length polydispersity and then results in an almost monodisperse system as

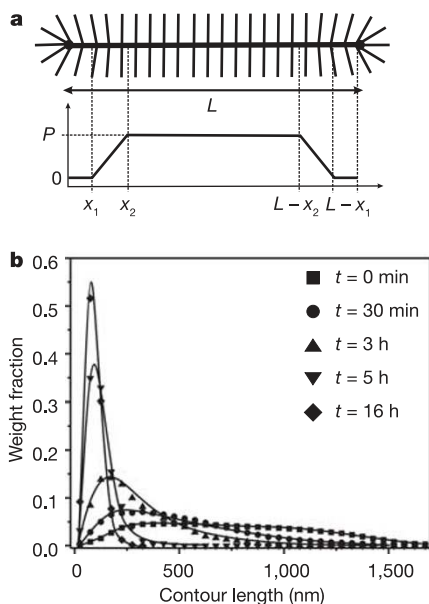


Figure 4 | Computer simulation of the scission process. **a**, The computer model assumes a constant scission probability P along most of the backbone; at the ends, P decays linearly to zero from $x_2 = 120$ nm to $x_1 = 40$ nm. This ensures the scission process stops at the experimentally observed $L_\infty = 40$ nm. **b**, Length distributions obtained by computer simulation for different time intervals t of the scission process (solid lines). The simulated distributions show good agreement with the distributions (data points) obtained by AFM on the same polymer/substrate system as used to obtain the images shown in Fig. 3a. The distributions are presented as the weight fraction of polymer chains of a certain number average contour length with a resolution (bin size) of 50 nm. The initial distribution function exactly corresponds to a realistic ensemble of 2,450 molecules acquired by AFM at $t = 0$ with $L_n = 496$ nm and $\text{PDI} = 1.52$.

the macromolecules gradually convert into short brush molecules that can no longer undergo scission. This behaviour can be simulated using a simple model wherein the probability P of bond scission occurring at any point along the backbone, except at the ends, is the same (Fig. 4a). Solid lines in Fig. 4b depict length distributions obtained at different durations of the computer-simulated scission process compare favourably with the corresponding length distributions measured by AFM (data points in Fig. 4b), giving good agreement between the modelled and experimentally measured polydispersity index. The simulated scission process eventually stops when all molecules become shorter than 80 nm, that is, in the range from $x_1 = 40$ nm and $2x_1 = 80$ nm.

Experiments are also being conducted to verify the effects of the substrate surface energy and the side-chain length on scission. As might be expected, preliminary findings show that backbone scission is very sensitive to small variations in both parameters. If surface energy is decreased to below 60 mN m^{-1} by adding more propanol to the water/propanol mixture used as substrate, molecules with long side chains ($n = 140$) that readily break on a 99.8/0.2 wt/wt% water/propanol surface ($\gamma = 69 \text{ mN m}^{-1}$) remain intact. Sharp retardation of the scission process was also observed upon shortening of the side chains: when using the same substrate (that is, a 99.8/0.2 wt/wt% water/propanol mixture) but pBA brush-like molecules with $n = 130$ ($d = 120$) instead of $n = 140$ does not lead to any noticeable shortening within reasonable experimental times (for example, days). However, we found that these molecules break on graphite, which has a slightly higher surface energy and a spreading parameter (Supplementary Fig. 1).

The essential feature of the bond scission observed here is that it occurs spontaneously upon adsorption onto a substrate. Linear and weakly branched polymer chains are obviously not at risk of chemical degradation upon surface adsorption; but all highly branched macromolecules that physically cannot allow all their monomeric units to interact with a substrate will be susceptible. In such cases, the load imposed by the adsorption forces is unevenly distributed over different structural elements of the molecular architecture according to the branching topology. In the system we studied, tension is concentrated along the backbone of molecular brushes and can be enough to break covalent carbon–carbon bonds. In the case of regular dendrimers, tension will focus at the covalent bonds near the principal branching centre of the dendrimers and, if the adsorption forces are strong enough, can cause the dendrimers to break. This essentially geometric effect is closely related to the observation that dendrimer polymerization stops above a certain generation, owing to the overcrowded molecular volume²³. These steric constraints can be eased by increasing the length of the spacer between branches in dendrimers, and between side chains in cylindrical brushes.

However, these structural modifications that make the branched structure looser also increase the 'footprint' of the adsorbed macromolecule, which in turn leads to a greater tensile force. Thus, with the current pursuit of new macro- and supramolecular materials that are specifically tailored for various surface applications, the surface-induced scission of covalent bonds will need to be considered carefully when designing complex molecular architectures. But in addition to emphasizing the need for designing 'stress-free' macromolecules for some applications, the phenomenon described here also opens up intriguing opportunities for deliberately designing architectures that break at pre-defined sites.

METHODS

Polymer characterization. Average molecular weights and molecular weight distribution of brush-like macromolecules were measured by gel permeation chromatography (GPC) equipped with Waters microstyragel columns (pore sizes 10^5 , 10^4 and 10^3 Å) and three detection systems: a differential refractometer (Waters Model 410), multi-angle laser light-scattering (MALLS) detector (Wyatt, DAWN EOS), and a differential viscometer (WGE Dr. Bures, η -1001).

In addition, we used a newly developed approach based on a combination of AFM and Langmuir–Blodgett techniques²⁴. This combination of methods ensured relative experimental errors in determining the polymerization degrees of the backbone and side chains below 5% and 10%, respectively.

Langmuir–Blodgett monolayers. To study the kinetics of the scission process, brush-like macromolecules with pBA side chains were adsorbed onto a surface of a water/propanol (99.8/0.2 wt/wt%) substrate. Propanol was chosen for its low surface energy and because its vapour pressure is nearly equivalent to that of water. This was necessary for long incubation times so that any subphase evaporation would lead to a minimal change in the surface energy. The evaporation of the subphase was closely monitored and controlled in an environmental chamber. For AFM analysis, the monolayer films were transferred onto a mica substrate at a controlled transfer ratio of 0.98, using the Langmuir–Blodgett technique. The surface tension of the substrate and the corresponding spreading parameter were measured by the Wilhelmy plate method.

Atomic force microscopy. Topographic images of individual molecules were collected using an atomic force microscope (Veeco Metrology Group) in tapping mode. We used silicon cantilevers (Mikromasch-USA) with a resonance frequency of about 140 kHz and a spring constant of about 5 N m. The radius of the probe was less than 10 nm. The analysis of digital images was performed using a custom software program (PEN) developed in-house and available from S.S.S. The program identifies the molecular contour and is capable of determining the contour length, the end-to-end distance, and the curvature distribution, all required for evaluation of the persistence length. For every sample, about ten images of about 300 molecules, that is, a total of 3,000 molecules were measured to ensure a relative standard error below 4% and an experimental error below 5% of the persistence length (Fig. 1), contour length, and polydispersity index (Fig. 3) measurements.

Received 17 August 2005; accepted 5 January 2006.

- Field, J. E. Mechanical and physical properties of diamond. *Inst. Phys. Conf. Ser.* **75**, 181–205 (1986).
- Derrington, A. Why diamonds top a hard league. *The Financial Times* n33034, section 3, pWFT2(1) (13/14 July 1996).
- Smith, P. & Lemstra, P. J. Tensile strength of highly oriented polyethylene. *J. Polym. Sci. Polym. Phys. Ed.* **19**, 1007–1009 (1981).
- Porter, R. S. & Kanamoto, T. A review on the tensile strength of polyethylene fibers. *Polym. Eng. Sci.* **34**, 266–268 (1994).
- Salvetat, J.-P. *et al.* Elastic and shear moduli of single-walled carbon nanotube ropes. *Phys. Rev. Lett.* **82**, 944–947 (1999).
- Yu, M.-F., Files, B. S., Arepalli, S. & Ruoff, R. S. Tensile loading of ropes of single wall carbon nanotubes and their mechanical properties. *Phys. Rev. Lett.* **84**, 5552–5555 (2000).
- De Gennes, P. G. Coil stretch transition of dilute flexible polymers under ultrahigh velocity gradients. *J. Chem. Phys.* **60**, 5030–5042 (1974).
- Harrington, R. E. & Zimm, B. H. Degradation of polymers by controlled hydrodynamic shear. *J. Phys. Chem.* **69**, 161–176 (1965).
- Odell, J. A., Keller, A. & Rabin, Y. Flow induced scission of isolated macromolecules. *J. Chem. Phys.* **88**, 4022–4028 (1988).
- Basedow, A. M. & Ebert, K. H. Ultrasonic degradation of polymers in solution. *Adv. Polym. Sci.* **22**, 83–148 (1977).
- Bensimon, A. *et al.* Alignment and sensitive detection of DNA by a moving interface. *Science* **265**, 2096–2098 (1994).
- Kishino, A. & Yanagida, T. Force measurements by micromanipulation of single actin filament by glass needles. *Nature* **334**, 74–76 (1988).
- Evans, E. Probing the relation between force—lifetime—and chemistry in single molecular bonds. *Annu. Rev. Biophys. Biomol. Struct.* **30**, 105–128 (2001).
- Smith, S. B., Cui, Y. & Bustamante, C. Overstretching B-DNA: The elastic response of individual double-stranded and single-stranded DNA molecules. *Science* **271**, 795–799 (1996).
- Cluzel, P. *et al.* DNA: An extensible molecule. *Science* **271**, 792–794 (1996).
- Mehta, A. D., Rief, M., Spudich, J. A., Smith, D. A. & Simmons, R. M. Single-molecule biomechanics with optical methods. *Science* **283**, 1689–1695 (1999).
- Sun, F., Sheiko, S. S., Moller, M., Beers, K. & Matyjaszewski, K. Conformational switching of molecular brushes in response to the energy of interaction with the substrate. *J. Phys. Chem. A* **108**, 9682–9686 (2004).
- Matyjaszewski, K. & Xia, J. Atom transfer radical polymerization. *Chem. Rev.* **101**, 2921–2990 (2001).
- Xu, H. *et al.* Molecular motion in a spreading precursor film. *Phys. Rev. Lett.* **93**, 206103 (2004).
- Neugebauer, D., Sumerlin, B., Matyjaszewski, K., Goodhart, B. & Sheiko, S. S. How dense are cylindrical brushes grafted from a multifunctional macroinitiator? *Polymer* **45**, 8173–8179 (2004).
- Austin, R. H., Brody, J. P., Cox, E. C., Duke, T. & Volkmuth, W. Stretch genes. *Phys. Today* 32–38 (February 1997).
- Sheiko, S. S. & Möller, M. Visualization of molecules—a first step to manipulation and controlled response. *Chem. Rev.* **101**, 4099–4123 (2001).
- Boris, D. & Rubinstein, M. A self-consistent mean field model of a starburst dendrimer: dense core vs. dense shell. *Macromolecules* **29**, 7251–7260 (1996).
- Sheiko, S. S. *et al.* Measuring molecular weight by atomic force microscopy. *J. Am. Chem. Soc.* **125**, 6725–6728 (2003).

Supplementary Information is linked to the online version of the paper at www.nature.com/nature.

Acknowledgements We thank E. T. Samulski and I. LaRue for their interest and discussions. This work was supported by grants from the National Science Foundation.

Author Contributions All authors contributed equally to this work.

Author Information Reprints and permissions information is available at npg.nature.com/reprintsandpermissions. The authors declare no competing financial interests. Correspondence and requests for materials should be addressed to S.S.S. (sergei@email.unc.edu).